Journal of Engineering Mathematics **40:** 269–282, 2001.

The influence of variable surface tension on capillary-gravity waves

E. OZUGURLU[1] and J.-M. VANDEN-BROECK[2]
[1]*Department of Mathematics and Center for the Mathematical Sciences, University of Wisconsin-Madison, WI 53706, U.S.A.*
[2]*School of Mathematics, The University of East Anglia, Norwich NR4 7TJ, U.K.*

Received 24 September 1998; accepted in revised form 22 August 2000

Abstract. Periodic gravity-capillary waves propagating at a constant velocity at the surface of a fluid of infinite depth are considered. The surface tension is assumed to vary along the free surface. A numerical procedure is presented to solve the problem with an arbitrary distribution of surface tension on the free surface. It is found that there are many different families of solutions. These solutions generalize the classical theory of gravity-capillary waves with constant surface tension. An asymptotic solution is presented for a particular distribution of variable surface tension.

Key words: variable surface tension, water waves, capillary-gravity waves

1. Introduction

Gravity-capillary waves have very interesting properties. In particular there are many different families of solutions characterized by dimples on their free surface. It is usual to study these waves by assuming that the surface tension is constant. The purpose of this paper is to show that the properties of gravity capillary waves remain qualitatively similar when the surface tension is variable along the free surface.

Gravity-capillary waves with constant surface tension have been studied since the beginning of the century. The evidence of multiple solutions was first shown by Harrisson [1] and Wilton [2] who included surface tension in Stokes's classical expansion for pure gravity waves. This work was later extended by Pierson and Fife [3], Nayfeh [4], Chen and Saffman [5] and others. Fully nonlinear numerical solutions were obtained by Schwartz and Vanden-Broeck [6], Chen and Saffman [7] and Hogan [8].

There are physical situations in which the surface tension is variable along a free surface. For example the variation in surface tension might be due to a non-uniformity of the temperature or the presence of surfactants. Here we do not study how a particular distribution of variable surface might occur. We look at the general problem of periodic waves with variable surface tension. Then the equations force the surface tension to be a periodic function which can therefore be represented as a Fourier series. We derive a numerical procedure which incorporates this Fourier representation. In this approach all the coefficients in this Fourier series are free parameters whose values we can choose. We present numerical results for some typical values of these parameters. The results include as a particular case the findings of Vanden-Broeck [9] for pure capillary waves.

Vanden-Broeck [9] showed that there are symmetric and nonsymmetric waves with variable surface tension. For simplicity we restrict our attention to symmetric waves. We show that gravity-capillary waves with variable surface tension have properties very similar to those with constant surface tension. Firstly, the linear theory predicts that there is a minimum speed below which periodic waves fail to exist. Secondly, there are many different families of nonlinear waves. We show that this multiplicity of solutions arises, like in the theory with constant surface tension, from the fact that two linear waves whose wavenumbers are multiples of each other can travel at the same speed. When the ratio of the wavenumbers is 2, the resulting nonlinear waves are referred to as Wilton's ripples. We present a semi-analytical theory of Wilton's ripples with arbitrary variable surface tension. In addition we derive an asymptotic expansion for a particular distribution of surface tension.

The formulation and the numerical procedure are similar to those presented in Vanden-Broeck [9]. A brief description is given in Section 2 and the reader is referred to Vanden-Broeck [9] for further details. The numerical results are presented in Sections 3 and 4. The asymptotic expansion is derived in Section 5. An important question is how the gradient of surface tension is maintained. This is addressed at the end of Section 2, where we discussed the relation between the inviscid flows presented in this paper and the corresponding slightly viscous flows.

2. Formulation and numerical procedure

We consider a train of periodic waves with wavelength λ traveling to the left at a constant phase velocity c. The fluid is inviscid, incompressible and of infinite depth. The flow is assumed to be irrotational. We introduce a frame of reference moving with the wave, with the origin at a trough and the y axis directed vertically upwards. As $y \to -\infty$, the velocity approaches c. Gravity is acting in the negative y direction (see Figure 1).

We introduce the complex potential $f = \phi + i\psi$ and choose $f = 0$ at $x = 0$. As discussed in the introduction, there are non-symmetric solutions. For simplicity we shall restrict our attention to waves which are symmetric with respect to $x = y = 0$.

We denote by u and v the horizontal and vertical components of the velocity. The basic equations can be written as (see for example Crapper [10] for a derivation)

$$\phi_{xx} + \phi_{yy} = 0, \tag{1}$$

$$\phi_y = \phi_x \eta_x \quad \text{on} \quad y = \eta(x), \tag{2}$$

$$\tfrac{1}{2}({\phi_x}^2 + {\phi_y}^2) + gy + \frac{T}{\rho}K = B \qquad \text{on} \qquad y = \eta(x), \tag{3}$$

$$\phi \to cx \qquad \text{as} \qquad y \to -\infty, \tag{4}$$

$$\phi(x+\lambda, y) = c\lambda + \phi(x, y), \qquad \eta(x+\lambda) = \eta(x). \tag{5}$$

Here g is the acceleration of gravity, T the surface tension, ρ the density, K the curvature and B the Bernoulli constant. The function $y = \eta(x)$ describes the shape of the free surface. Equation (1) is Laplace's equation to be satisfied in the flow domain. Equations (2) and (3) are the kinematic and dynamic boundary conditions on the free surface. The conditions (5) impose the periodicity of the flow and (4) forces the flow to approach a uniform stream with constant velocity c as $y \to -\infty$.

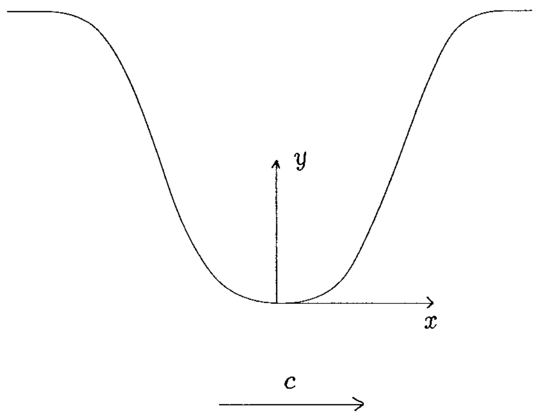

Figure 1. Sketch of the flow and the coordinates. Only one wavelength of the wave is shown. As $y \to -\infty$, the flow is uniform with constant velocity c.

We assume a variable surface tension along the free surface. Equations (3) and (5) imply that T is then a periodic function of x, *i.e.*

$$T(x + \lambda) = T(x). \tag{6}$$

The problem defined by (1–5) is difficult to solve for two reasons. The first is that the boundary condition (3) is nonlinear. The second is that the shape of the boundaries (*i.e.* the function $y = \eta(x)$) has to be found as part of the solution. As shown by Stokes, this second difficulty can be avoided by taking ϕ and ψ as independent variables. The flow domain is then mapped from the (x, y)-plane of Figure 1 to the lower half plane of the (ϕ, ψ)-plane. All the quantities x, y, u and v are considered as functions of f. Relations (5) imply that there are periodic in ϕ with period $c\lambda$. From (6), it then follows that T is a periodic function of ϕ with period $c\lambda$. The assumed symmetry of the wave about $\phi = \psi = 0$ implies that T is an even function of ϕ. We therefore represent T as a Fourier cosine series, *i.e.*

$$T = T_0 \left[1 + \sum_{n=1}^{\infty} a_n \cos\left(\frac{nk\phi}{c} \right) \right]. \tag{7}$$

Here $k = 2\pi/\lambda$ is the wavenumber and T_0 is a constant.

This completes the formulation of the problem. We seek $u - \mathrm{i}v$ as an analytic function of f, periodic in ϕ with period $c\lambda$. This function must approach c as $\psi \to -\infty$ and satisfy (3) on $\psi = 0$.

To solve the problem numerically, we introduce dimensionless variables by choosing λ as the unit length and c as the unit velocity. Next we define $\tau - \mathrm{i}\theta$ by

$$u - \mathrm{i}v = \mathrm{e}^{\tau - \mathrm{i}\theta} \tag{8}$$

Following Vanden-Broeck [9], we rewrite (3) as

$$\frac{\mathrm{e}^{2\tau}}{2} + \gamma y - \alpha \left[1 + \sum_{n=1}^{\infty} a_n \cos(2\pi n\phi) \right] \mathrm{e}^{\tau} \frac{\partial\theta}{\partial\phi} = B, \tag{9}$$

where

$$\gamma = \frac{g\lambda}{c^2} \qquad \text{and} \qquad \alpha = \frac{T_0}{\rho\lambda c^2}. \tag{10}$$

Using the periodicity of the wave and the condition $u - \mathrm{i}v \to 1$ as $\psi \to -\infty$, we write

$$\tau - \mathrm{i}\theta = \sum_{n=1}^{\infty} u_n \mathrm{e}^{-2\mathrm{i}\pi n f}, \tag{11}$$

where the coefficients u_n are real because of the assumed symmetry with respect to $\phi = 0$.

Since $u - \mathrm{i}v = \mathrm{d}f/\mathrm{d}z$,

$$\frac{\partial x}{\partial \phi} + \mathrm{i}\frac{\partial y}{\partial \phi} = \frac{1}{u - \mathrm{i}v} = \mathrm{e}^{-\tau + \mathrm{i}\theta}. \tag{12}$$

Integrating (12) we rewrite (9) as

$$\frac{\mathrm{e}^{2\tau}}{2} + \gamma \int_0^{\phi} \mathrm{e}^{-\tau} \sin\theta \, \mathrm{d}\phi - \alpha \left[1 + \sum_{n=1}^{\infty} a_n \cos(2\pi n \phi) \right] \mathrm{e}^{\tau} \frac{\partial \theta}{\partial \phi} = B. \tag{13}$$

Following Vanden-Broeck [9], we solve the problem numerically by truncating the infinite series in (13) after $N - 1$ terms. We find $N + 2$ unknowns $u_1, u_2, ..., u_{N-1}, \gamma, \alpha$ and B by collocation. We introduce the N mesh points

$$\phi_I = \frac{1}{2N}(I - 1), \qquad I = 1, \ldots, N. \tag{14}$$

By satisfying (13) at the mesh points (14), we obtain N nonlinear algebraic equations. The integral in (13) is evaluated numerically. An extra equation is obtained by fixing the steepness s of the wave (*i.e.* the difference of height between a crest and a trough divided by the wavelength).

Using (12), we write this equation as

$$\int_0^{\frac{1}{2}} \mathrm{e}^{-\tau} \sin\theta \, \mathrm{d}\phi = s, \tag{15}$$

where s is given. The integral in (15) is also evaluated numerically.

To derive the last equation we first introduce the capillary number

$$\kappa = 4\pi^2 \frac{T_0}{\rho g \lambda^2} \tag{16}$$

and the gravity parameter

$$\mu = 2\pi \frac{c^2}{g\lambda}. \tag{17}$$

The parameters κ, α and γ are related by the identity

$$\kappa = 4\pi^2 \frac{\alpha}{\gamma}. \tag{18}$$

The last equation is given by (18) where the left-hand side is given.

This system of $N + 2$ nonlinear equations with $N + 2$ unknowns is solved by Newton's method.

After finding the coefficients u_n, the free-surface profile is obtained in the parametric form $x = x(\phi)$, $y = y(\phi)$ by integrating numerically (12). We note that (7) defines T as a function of ϕ. This is an inverse formulation and T as a function of x is defined at the end of the calculations by (7) and $x = x(\phi)$.

For $\gamma = 0$, the scheme reduces to the one used by Vanden-Broeck [9].

Let us mention that there is a variation of the numerical procedure in which the integral in (13) is avoided. The idea is to differentiate (13) with respect to ϕ. This leads

$$e^{2\tau}\frac{\partial \tau}{\partial \phi} + \gamma e^{-\tau}\sin\theta - \alpha\frac{\partial}{\partial \phi}\left[\left[1 + \sum_{n=1}^{\infty} a_n \cos(2\pi n\phi)\right] e^{\tau}\frac{\partial \theta}{\partial \phi}\right] = 0. \tag{19}$$

The numerical procedure is then the same but with this new equation instead of (13). Both numerical schemes were found to give equivalent results.

Before concluding this section, we discuss how the inviscid solutions presented in this paper might approximate a slightly viscous flow (or more precisely a flow with high Reynolds number). For viscous flows, an extra boundary condition needs to be satisfied on the free surface, namely

$$\frac{d}{dx}\frac{T}{\rho\lambda c^2} = \frac{1}{R}(\frac{\partial v}{\partial x} + \frac{\partial u}{\partial y}), \tag{20}$$

where

$$R = \frac{c\lambda}{\nu}. \tag{21}$$

Here ν is the kinematic viscosity (see Lucassen-Reynders and Lucassen [11] for a derivation).

For constant T and $\nu \neq 0$, (20) implies that the tangential stress vanishes on the free surface. For slightly viscous fluid and constant T, we can solve the flow problem approximately by first constructing an inviscid solution (not satisfying (20)). In a second stage, a boundary-layer solution is then constructed near the free surface where the tangential stress varies from its inviscid value

$$\frac{1}{R}\left(\frac{\partial v}{\partial x} + \frac{\partial u}{\partial y}\right) \tag{22}$$

to zero (see Batchelor [12], pp. 364).

We propose to approximate the problem with variable surface tension in a similar way. First we solve the inviscid problem ignoring (20). These are the solutions presented in this paper. Then a boundary-layer solution can be added near the free surface where the tangential stress varies from its inviscid value (22) to the value

$$\frac{d}{dx}\frac{T}{\rho\lambda c^2} \tag{23}$$

predicted by (20). We note that our approach reduces to the classical one presented in Batchelor [12] when T is constant. The boundary layer is not constructed here but the above argument suggests that the inviscid solutions calculated in this paper provide a good approximation for slightly viscous fluids away from a thin boundary layer near the free surface.

3. Linear theory

We can gain some preliminary insight into the problem by linearizing the equations around a uniform stream.

Assuming $\tau \ll 1$ and $\theta \ll 1$ we linearize (19) as

$$\frac{\partial\tau}{\partial\phi} + \gamma\theta - \alpha\frac{\partial}{\partial\phi}\left[\left[1 + \sum_{n=1}^{\infty} a_n \cos(2\pi n\phi)\right]\frac{\partial\theta}{\partial\phi}\right] = 0. \tag{24}$$

When $a_n = 0$ (*i.e.* for constant surface tension), the problem has an exact solution

$$\tau - \mathrm{i}\theta = A\mathrm{e}^{-2\mathrm{i}\pi f}, \qquad \mu = 1 + \kappa. \tag{25a,b}$$

Here A is a constant.
Using (17) and (18), we can rewrite (25b) as

$$c^2 = \frac{g\lambda}{2\pi} + \frac{T_0}{\rho}\frac{2\pi}{\lambda}. \tag{26}$$

Equation (26) is the familiar dispersion relation of linear gravity-capillary waves.

To describe the results further, it is convenient to introduce the new parameters

$$\bar{c} = \frac{\mu^{1/2}}{\kappa^{1/4}} = \frac{c}{\left(\frac{gT_0}{\rho}\right)^{1/4}} \qquad \text{and} \qquad \bar{\lambda} = 2\pi\kappa^{-1/2} = \frac{\lambda}{\left(\frac{T_0}{\rho g}\right)^{1/2}}. \tag{27}$$

The parameters $\bar{c}$ and $\bar{\lambda}$ can be viewed as the dimensionless velocity and the dimensionless wavelength if we choose $(gT_0/\rho)^{1/4}$ as the unit velocity and $(T_0/\rho g)^{1/2}$ as the unit length.
Using (27) we rewrite (26) as

$$\bar{c}^2 = \frac{\bar{\lambda}}{2\pi} + \frac{2\pi}{\bar{\lambda}}. \tag{28}$$

Relation (28) is shown graphically in Figure 2 where we plot values of $\bar{c}^2$ versus $\bar{\lambda}$ (see solid curve). When $\bar{\lambda} = 2\pi$, $\bar{c}^2$ has a minimum.

When $a_n \neq 0$, we no longer have an exact solution because the linear problem has variable coefficients. Therefore we solve the linear problem numerically by the scheme of Section 2 with (13) replaced by (24). The coefficients u_n were found to decrease rapidly. For example $u_1 \approx 0{\cdot}1047$, $u_2 \approx -0{\cdot}0856, \ldots, u_{78} \approx 0{\cdot}0000000174$ for $a_8 = 0{\cdot}15$, $a_j = 0$, $j \neq 8$ and $\kappa = 0{\cdot}5$.

Numerical values of $\bar{c}^2$ versus $\bar{\lambda}$ are shown in Figure 2 for $a_8 = 0{\cdot}15$ and $a_8 = 0{\cdot}45$. As a_8 increases the curve moves down. Figure 2 shows that the relation between $\bar{c}$ and $\bar{\lambda}$ for variable surface tension is similar to that with constant surface tension. In particular, the three curves of Figure 2 have a minimum. This behavior does not depend on the particular choice $a_8 \neq 0$, $a_j = 0$, $j \neq 8$ and similar results were found for other values of a_n.

A consequence of the existence of minima in Figure 2 is that waves of different wavelengths can travel at the same speed. In particular a wave of wavelength $\bar{\lambda}$ and a wave whose wavelength is $\bar{\lambda}/m$ (where m is an integer) can travel at the same speed if $\kappa = (2\pi/\bar{\lambda})^2$ is equal to some critical value κ_m.

When the surface tension is constant (*i.e.* $a_n = 0$ for all n), κ_m can be calculated analytically as follows. Using (28), we see that waves of wavelength $\bar{\lambda}$ and $\bar{\lambda}/m$ travel at the same speed if

$$\frac{\bar{\lambda}}{2\pi} + \frac{2\pi}{\bar{\lambda}} = \frac{\bar{\lambda}}{2\pi m} + \frac{2\pi m}{\bar{\lambda}}. \tag{29}$$

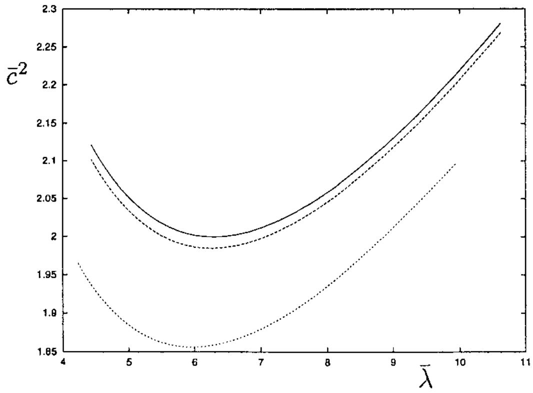

Figure 2. Values of $\bar{c}^2$ versus $\bar{\lambda}$. Here $\bar{c}$ and $\bar{\lambda}$ are the dimensionless velocity and the dimensionless wavelength defined in (27). The curves from top to bottom correspond to $a_8 = 0$, $a_8 = 0{\cdot}15$ and $a_8 = 0{\cdot}45$ with $a_j = 0$, $j \neq 8$. The three curves have a minimum.

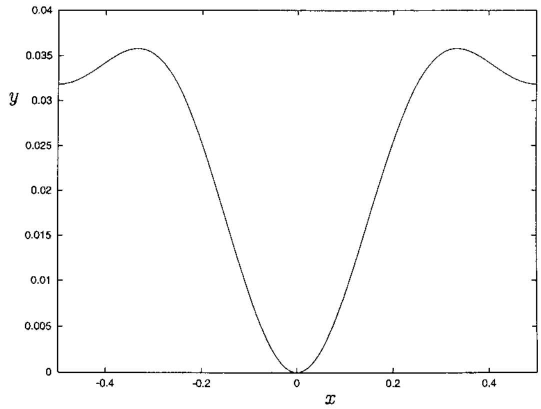

Figure 3. Free surface profile of a Wilton ripple with $D = A$ in (31). Here $A = 0.1$. Only one wavelength is shown.

Relation (27) and (29) give

$$\kappa_m = \frac{1}{m}. \tag{30}$$

When the surface tension is variable (*i.e.* $a_n \neq 0$), κ_m cannot generally be calculated analytically. Therefore we present at the end of this section a numerical procedure to evaluate κ_m.

For $\kappa = \kappa_m$ and constant surface tension, the solution (25a) is incomplete and the general solution of the linear problem is

$$\tau - \mathrm{i}\theta = A\mathrm{e}^{-2\mathrm{i}\pi f} + D\mathrm{e}^{-2\mathrm{i}\pi m f}, \tag{31}$$

where A and D are constants. The value of D cannot be determined within the framework of the linear theory. To find D, we need to use a nonlinear theory, *i.e.* use (19) instead of (24). For constant surface tension, Wilton [2] found $D = \pm A$ for $\kappa = \kappa_2 = \frac{1}{2}$. His calculation was based on an expansion in powers of the amplitude of the wave. There are two 'Wilton ripples' corresponding to $D = A$ and $D = -A$. One has a crest dimple and the other a trough dimple. There are shown in Figures 3 and 4 for $A = 0{\cdot}1$.

For $\kappa = \kappa_m$ and variable surface tension, the general solution of the linear problem can be written as

$$\tau - \mathrm{i}\theta = AL_1(f) + DL_2(f), \tag{32}$$

where $L_1(f)$ and $L_2(f)$ are, respectively, the two linear solutions of wavelengths $\bar{\lambda}$ and $\bar{\lambda}/m$. We note that for constant surface tension $L_1(f) = \mathrm{e}^{-2\mathrm{i}\pi f}$ and $L_2(f) = \mathrm{e}^{-2\mathrm{i}\pi m f}$, so that (32) reduces to (31).

We conclude this section by describing the procedure to compute κ_m when the surface tension is variable . For simplicity we assume $m = 2$. We consider two linear waves whose

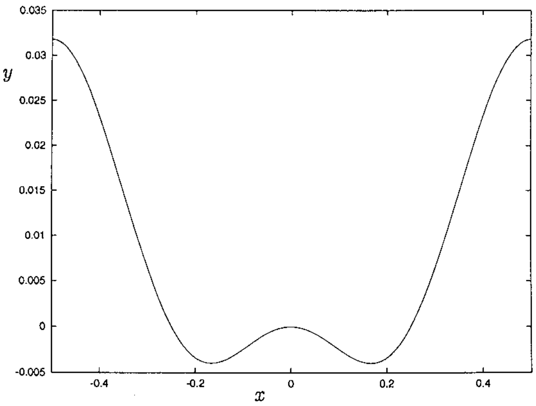

Figure 4. Same as Figure 3 with $D = -A$.

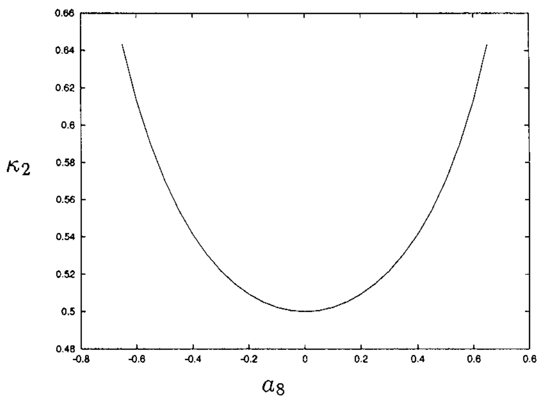

Figure 5. Values of the critical capillary number κ_2 versus a_8 with $a_j = 0$, $j \neq 8$. The variable surface tension is defined by (7).

ratio of the wavelengths is equal to 2 (*i.e.* $L_1(f)$ and $L_2(f)$). In dimensionless variables they are represented by the expansions (11) and

$$\tau' - \mathrm{i}\theta' = \sum_{n=1}^{\infty} u_n' \mathrm{e}^{-2\mathrm{i}\pi n f}. \tag{33}$$

We require (11) to satisfy (24) and (33) to satisfy a modification of (24) (denoted by (24′)) obtained by replacing with γ and α by the new parameters $\bar{\gamma}$ and $\bar{\alpha}$. These new parameters satisfy

$$\frac{\bar{\alpha}}{\bar{\gamma}} = 4\frac{\alpha}{\gamma} \quad \text{and} \quad \bar{\gamma}\bar{\alpha} = \gamma\alpha. \tag{34, 35}$$

Relations (34) and (35) express the facts that the ratio of the wavelengths is equal to 2 and that the waves travel at the same speed. We truncate the infinite series in (11) and (33) after N terms and satisfy (24) and (24′) at the mesh points (14). This yield $2N$ equations for the $2N + 4$ unknowns $u_1, u_2, \ldots, u_N, u_1', u_2', \ldots, u_N', \alpha, \gamma, \bar{\alpha}$ and $\bar{\gamma}$. Relations (34) and (35) provide two more equations. We obtained the last two equations by fixing the steepness of the waves. We note that the numerical results are independent of the actual values chosen for the steepness since the problem is linear. This system of algebraic equations is solved by Newton's method. The value of κ_2 is then given by

$$\kappa_2 = \frac{4\pi^2\alpha}{\gamma}. \tag{36}$$

Values of κ_2 versus a_8 with $a_j = 0$, $j \neq 8$ are shown in Figure 5.

We note that the scheme gives in addition to the value of κ_2, the two linear solutions $L_1(f)$ and $L_2(f)$. These solutions will be useful for the theory of Wilton's ripples presented in the next section.

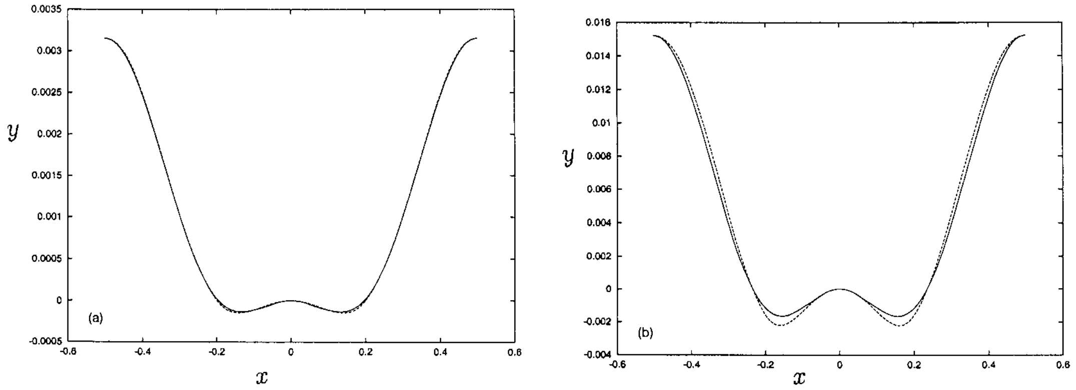

Figure 6. Free surface profiles for $a_8 = 0{\cdot}15$, $a_j = 0$, $j \neq 8$ and $s = 0{\cdot}0032$ (Figure 6a), $s = 0{\cdot}0153$ (Figure 6b) and $s = 0{\cdot}028$ (Figure 6c). Here s is equal to the ordinates of the crests. The solid curves are the nonlinear solutions and the broken curves correspond to the right-hand side of (37).

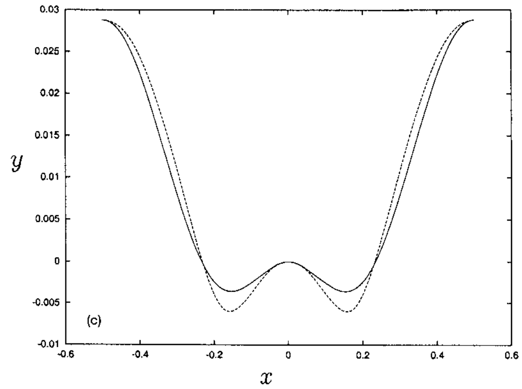

Figure 6. Continued.

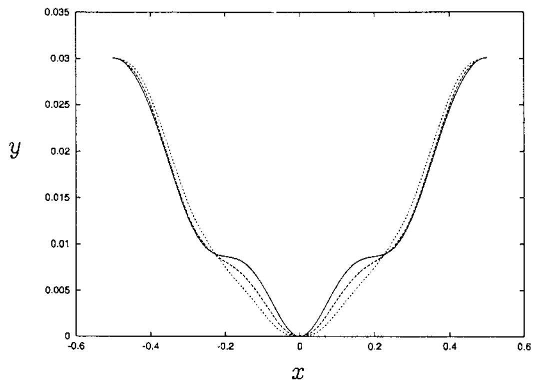

Figure 7. Free surface profiles for $\kappa = 0{\cdot}33$, $a_j = 0$, $j \neq 8$ and $a_8 = 0$ (solid curve), $a_8 = 0{\cdot}15$ (broken curve) and $a_8 = 0{\cdot}30$ (dotted line).

4. Nonlinear theory

We used the numerical scheme of Section 2 to compute solutions for various values of s, a_n and κ. The coefficients u_n were found to decrease rapidly as n increases. For example $u_1 \approx 0{\cdot}02239$, $u_2 \approx -0{\cdot}0162$, ..., $u_{78} \approx 0{\cdot}00000002$ for $a_8 = 0{\cdot}15$, $a_j = 0$, $j \neq 8$, $\kappa = 0{\cdot}5$ and $s = 0{\cdot}007$.

First we checked the scheme by reproducing the results of Schwartz and Vanden-Broeck [6] for constant surface tension . Next we used the scheme to generalize the Wilton ripples (*i.e.* waves for $\kappa = \kappa_2$) to the case of variable surface tension. Here we present typical results for $a_8 \neq 0$ and $a_j = 0$ for $j \neq 8$. For a given values of a_8, the corresponding value of κ_2 can be calculated by the scheme described at the end of Section 3 (see Figure 5). We then compute a nonlinear solution for these values of a_8 and κ by the scheme of Section 2. We denote the computed values of $\tau - i\theta$ by $Nl(f)$. In the limit as $s \to 0$, we expect that

$$Nl(f) \to AL_1(f) + DL_2(f), \tag{37}$$

where $L_1(f)$ and $L_2(f)$ are the two linear solutions calculated at the end of Section 3. To check (37) we find A and D by imposing two conditions. The first is that $Nl(f)$ and $AL_1(f)+DL_2(f)$ have the same steepness. The second is that

$$\int_o^{\lambda/2} [Nl(\phi) - AL_1(\phi) - BL_2(\phi)]^2 \mathrm{d}\phi \tag{38}$$

is minimum. The last condition imposes that the difference between the right- and left-hand sides of (37) is minimum in the L_2 norm. We can now compare the right- and left-hand sides of (37). Typical results for $a_8 = 0{\cdot}15$, $a_j = 0$, $j \neq 8$ are shown in Figure 6. The solid curve corresponds to $Nl(f)$ and the broken curve to $AL_1(f) + DL_2(f)$. The results show that the agreement between the solid and broken curve improves as the steepness s is decreased. Since we chose the origin at the through, the steepness is simply the ordinate of the crests. This constitutes a check on (37) and on the various numerical procedures.

Finally we present in Figure 7, numerical results for $\kappa = 0{\cdot}33$ and various values of a_8, $a_j = 0$, $j \neq 8$. Here we found that the dimples are less pronounced and that the wave is getting flatter near the trough as we increase a_8.

5. Perturbation results

In the previous sections, the surface tension is a prescribed (periodic) function of ϕ. The numerical procedures can be extended to cases in which the surface tension is prescribed as a function of other quantities along the free surface. As an example we present in this section results for a variable surface tension which depends on the curvature of the free surface. More precisely we replace (7) by

$$T = T_0[1 - \tilde{\epsilon}K], \tag{39}$$

where $\tilde{\epsilon}$ is a given constant. The numerical procedure of Section 2 applies unchanged if we replace the square bracket in (9) by

$$\left[1 + \frac{\tilde{\epsilon}}{\lambda} e^{\tau} \frac{\partial\theta}{\partial\phi}\right]. \tag{40}$$

We denote this equation by (9′) The linearization of (9′) is (24) with $a_n = 0$ for all n. In other words the linearization of (9′) is the classical linear problem with constant surface tension whose solution is given by (25a) and (25b). This nice property suggests that for the variable surface tension (39), it should be easy to improve on the linear theory by constructing an expansion in powers of the amplitude of the wave. This is achieved up to second order in this section. This provides us with some analytical results to supplement the numerical calculations presented in the previous sections.

Since we are only calculating solutions up to second order in the amplitude, it is more convenient to use Cartesian coordinates instead of the variables ϕ and ψ.

The governing equations in dimensional variables are then (1), (2), (4), (5) and

$$\frac{1}{2}({\phi_x}^2+{\phi_y}^2)+gy-\frac{T_0}{\rho}\left[1+\tilde{\epsilon}\frac{\eta_{xx}}{(1+{\eta_x}^2)^{3/2}}\right]\frac{\eta_{xx}}{(1+{\eta_x}^2)^{3/2}}=\frac{1}{2}c^2 \quad \text{on} \quad y=\eta(x). \tag{41}$$

Here we chose the origin of y such that the Bernoulli constant is $c^2/2$.

We seek a solution in the form of an expansion in powers of a small parameter ϵ. Thus we write

$$\eta(x) \quad = \epsilon\eta_1(x)+\epsilon^2\eta_2(x)+\cdots, \tag{42}$$

$$\phi(x,y)=cx+\epsilon\phi_1(x,y)+\epsilon^2\phi_2(x,y)+\cdots, \tag{43}$$

$$c=c_0+\epsilon c_1+\epsilon^2 c_2+\cdots, \tag{44}$$

The parameter ϵ is a measure of the wave amplitude. Here we define it as $\epsilon = ak$ where a is the first Fourier coefficient of $\eta(x)$.

Substituting (42)–(44) in (1), (2), (4), (5) and (41) and equating the coefficients of ϵ, we obtain

$$\phi_{1xx}+\phi_{1yy}=0, \tag{45}$$

$$\phi_{1y}=c_0\eta_{1x} \quad \text{on} \quad y=0, \tag{46}$$

$$c_0\phi_{1x}+g\eta_1-\frac{T_0}{\rho}\eta_{1xx}=0, \tag{47}$$

$$\phi_1\to 0 \quad \text{as} \quad y\to -\infty, \tag{48}$$

$$\phi_1(x+\lambda,y)=\phi_1(x,y), \quad \eta_1(x+\lambda)=\eta_1(x). \tag{49}$$

Similarly, equating the coefficients of ϵ^2, we obtain

$$\phi_{2xx}+\phi_{2yy}=0, \tag{50}$$

$$\phi_{2y}-c_0\eta_{2x}=-\phi_{1yy}\eta_1+(c_1+\phi_{1x})\eta_{1x} \quad \text{on} \quad y=0, \tag{51}$$

$$-\frac{T_0}{\rho}\eta_{2xx}+c_0\phi_{2x}+g\eta_2= \\ -c_0\phi_{1xy}\eta_1-c_1\phi_{1x}-\tfrac{1}{2}({\phi_{1x}}^2+{\phi_{1y}}^2)+\frac{T_0}{\rho}\tilde{\epsilon}{\eta^2}_{1xx} \quad \text{on} \quad y=0, \tag{52}$$

$$\phi_2\to 0 \quad \text{as} \quad y\to -\infty, \tag{53}$$

$$\phi_2(x+\lambda,y)=\phi_2(x,y), \quad \eta_2(x+\lambda)=\eta_2(x). \tag{54}$$

We note that (45–49) is the linear problem with constant surface tension.

We first assume that

$$\kappa\neq\frac{1}{m}. \tag{55}$$

As shown in Section 3, the solution of the linear problem (45–49) is unique and given by

$$\phi_1(x, y) \quad = -c_0 A_1 e^{ky} \sin(kx), \tag{56}$$

$$\eta_1(x) \quad = A_1 \cos(kx), \tag{57}$$

$$c_0{}^2 = \frac{g}{k} + \frac{T_0}{\rho} k, \tag{58}$$

where $k = 2\pi/\lambda$ is the wavenumber and A_1 is a constant. Here we chose $x = 0$ at a crest of the wave. The definition of ϵ implies that $A_1 = 1/k$.

Next we use separation of variables to write the solution of (50), (53) and (54) as

$$\phi_2(x, y) = \sum_{n=1}^{\infty} F_n \mathrm{e}^{nky} \sin(nkx) \tag{59}$$

and we seek $\eta_2(x)$ in the form

$$\eta_2(x) = E_0 + \sum_{n=2}^{\infty} E_n \cos(nkx). \tag{60}$$

We started the sum in (60) at $n = 2$ in accordance with our definition of ϵ

Substituting (59) and (60) in (51) and (52) and equating the constant terms in (51) and the coefficients of $\sin x$ and $\cos x$ in (51) and (52), we obtain

$$E_0 = \frac{T_0}{2\rho g} \tilde{\epsilon} A_1{}^2 k^4, \qquad k F_1 = -k c_1 A_1, \qquad k c_0 F_1 = k c_0 c_1 A_1. \tag{61, 62, 63}$$

Similarly, equating the coefficients of $\sin(2x)$ and $\cos(2x)$ in (51) and (52) yields

$$2k F_2 + 2k c_0 E_2 = k^2 c_0 A_1{}^2, \tag{64}$$

$$4k^2 E_2 \frac{T_0}{\rho} + g E_2 + 2k c_0 F_2 = \tfrac{1}{2} k^2 c_0{}^2 A_1{}^2 + \frac{1}{2} \frac{T_0}{\rho} \tilde{\epsilon} k^4 A_1{}^2. \tag{65}$$

Finally, by equating coefficients of $\sin(nx)$ and $\cos(nx)$ in (51) and (52) for $n = 3, 4, \cdots$ we have

$$nk F_n + nk c_0 E_n = 0, \tag{66}$$

$$n^2 k^2 E_n \frac{T_0}{\rho} + g E_n + nk c_0 F_n = 0. \tag{67}$$

Solution of (62–65) gives

$$F_1 = 0, \quad c_1 = 0 \tag{68}$$

and

$$E_2 = -\frac{1}{2k} \frac{c_0{}^2 - \frac{T_0}{\rho} \tilde{\epsilon} k^2}{(2k \frac{T_0}{\rho} - \frac{g}{k})}, \qquad F_2 = \frac{c_0 T_0}{2\rho} [\frac{3 - k\tilde{\epsilon}}{2k \frac{T_0}{\rho} - \frac{g}{k}}]. \tag{69, 70}$$

Here we have used $A_1 = 1/k$ and (58).

Eliminating F_n between (66) and (67), we get

$$\left[\left((nk)^2\frac{T}{\rho} + g - nkc_0{}^2\right)\right]E_n = 0. \tag{71}$$

Relations (66) and (67) imply

$$E_n = F_n = 0 \quad \text{for} \quad n = 3, 4, \ldots, \tag{72}$$

provided the square bracket in (71) is different from zero. This requirement is satisfied if (55) holds.

Up to second order the solution is defined by (42–44), where the various terms are given by (56–61), (68–70) and (72). We note that the denominators of the second-order approximation (69), (70) vanish when $\kappa = \frac{1}{2}$. Similar singularities in the higher-order terms occur when $\kappa = 1/m$. These singularities are related to the fact that the solution (56), (57) of the linear problem is incomplete when $\kappa = 1/m$.

We now examine in details the case $\kappa = 1/2$ (*i.e.* we develop a theory of the Wilton ripples for the variable distribution of surface tension (39)).

The complete solution of the linear problem is then

$$\phi_1(x, y) \quad = -c_0A_1\mathrm{e}^{ky}\sin(kx) - c_0A_2\mathrm{e}^{2ky}\sin(2kx), \tag{73}$$

$$\eta_1(x) \quad = A_1\cos(kx) + A_2\cos(2kx), \tag{74}$$

where c_0 is defined by (58). Relations (73), (74) are equivalent to (31). The difference is that the independent variables are ϕ and ψ in (31) and x and y in (73), (74). Following the analysis in the case $\kappa \neq 1/m$, we substitute (73) and (74) in the right-hand sides of (51) and (52) and we seek ϕ_2 and η_2 in the form (59) and (60). Equating the constant terms and the coefficients of $\sin x$, $\cos x$, $\sin 2x$, $\cos 2x, \ldots$. in (51) and (52) give equations for A_2, c_1, F_n and E_n. Here we present only the calculations leading to the determination of the constants A_2 and c_1 in the linear solution.

By equating the coefficients of $\sin x$ in (51) and of $\cos x$ in (52), we have

$$kF_1 = \tfrac{3}{2}k^2c_0A_1A_2 - kc_1A_1, \tag{75}$$

$$kc_0F_1 = \tfrac{1}{2}k^2c_0{}^2A_1A_2 + kc_0c_1A_1 + 4\frac{T_0}{\rho}\tilde{\epsilon}k^4A_1A_2. \tag{76}$$

Similarly, by equating the coefficients of $\cos 2x$ in (52) and $\sin 2x$ in (51) we have

$$2kF_2 + 2kc_0E_2 = k^2c_0A_1{}^2 - 2kc_1A_2, \tag{77}$$

$$4k^2E_2\frac{T_0}{\rho} + gE_2 + 2kc_0F_2 = \frac{1}{2}k^2c_0{}^2A_1{}^2 + 2kc_0c_1A_2 + \tfrac{1}{2}\frac{T_0}{\rho}\tilde{\epsilon}k^4A_1{}^2. \tag{78}$$

Solving (75–78) we get

$$c_1 = \tfrac{1}{2}kc_0A_2 - 2\frac{T_0}{\rho}\tilde{\epsilon}k^3\frac{A_2}{c_0} \tag{79}$$

and

$$A_2{}^2 = \frac{1}{4} A_1{}^2 \, \frac{c_0{}^2 - \dfrac{T_0}{\rho}\tilde{\epsilon} k^2}{c_0{}^2 - 4\dfrac{T_0}{\rho}\tilde{\epsilon} k^2}. \tag{80}$$

Relation (80) shows that A_2^2 increases as $\tilde{\epsilon}$ increases. Similarly, Equation (79) implies that $|c_1|$ decreases as $\tilde{\epsilon}$ increases.

Note that, when $\tilde{\epsilon} = 0$, we recover the relation

$$A_2 = \pm\tfrac{1}{2} A_1 \tag{81}$$

obtained by Wilton [2] for constant surface tension. The corresponding free-surface profiles are shown in Figures 3 and 4.

6. Conclusions

We have generalized the theory of periodic gravity capillary waves by allowing the surface tension to vary along the free surface. We have found that the linear theory predicts a minimum of the phase velocity. We have shown numerically and analytically that this minimum implies the existence of multiple solutions similar to the ones obtained for constant surface tension.

Acknowledgements

The work of the authors was supported in part by the National Science Foundation. The authors thank the referees for their constructive comments.

References

1. W. J. Harrison, The influence of viscosity and capillarity on waves of finite amplitude. *Proc. Lond Math. Soc.* 7 (1909) 107–121.
2. J. R. Wilton, On ripples. *Phil. Mag.* 29 (1915) 688–700.
3. W. J. Pierson and P. Fife, Some nonlinear properties of long–crested periodic waves with lengths near 2.44 centimeters. *J. Geophys. Res.* 66 (1961) 163–179.
4. A. H. Nayfeh, Finite amplitude surface waves in a liquid layer. *J. Fluid Mech.* 40 (1970) 671–684.
5. B. Chen and P. G. Saffman, Steady gravity-capillary waves on deep water-I. Weakly nonlinear waves. *Stud. Appl. Math.* 60 (1979) 183–210.
6. L. W. Schwartz and J.-M. Vanden-Broeck, Numerical solution of the exact equations for capillary-gravity waves. *J. Fluid Mech.* 95 (1979) 119–139.
7. B. Chen and P. G. Saffman, Steady gravity-capillary waves on deep water-II. Numerical results for finite amplitude. *Stud. Appl. Math.* 62 (1980) 95-111.
8. S. J. Hogan, Some effects of surface tension on steep water waves, Part 3. *J. Fluid Mech.* 110 (1981) 381–410.
9. J.-M. Vanden-Broeck, Capillary waves with variable surface tension. *Z. Angew. Math. Phys.* 47 (1996) 799–808.
10. G. D. Crapper, An exact solution for progressive capillary waves of arbitrary amplitude. *J. Fluid Mech.* 2 (1957) 532–540.
11. E.H. Lucassen-Reynders and J. Lucassen, Properties of capillary waves. *Adv. Colloid Interface Sci.* 2 (1969) 347–395.
12. G. K. Batchelor, *An Introduction to Fluid Dynamics.* Cambridge University Press (1967) 615pp.